

Combustion Behavior of Aluminum Particles in ADN/GAP Composite Propellants

Volker Weiser, Andrea Franzin, Luigi T. DeLuca, Sebastian Fischer, Volker Gettwert, Stefan Kelzenberg, Sebastian Knapp, Angelika Raab, Evelin Roth, and Norbert Eisenreich

Abstract Propellants containing ADN/GAP are regarded as a promising green alternative to AP/HTPB solid rocket propellants because of avoiding chloric acid emission. The addition of aluminum powder is a classical approach to increase the theoretical specific impulse of composite propellants. The optimum aluminum content is in the range of 16–18 % Al. But propellant formulations with ADN, a chlorine-free oxidizer, and GAP, an energetic binder, generate no chloric acid but more nitrogen on combustion achieving similar performance. Significantly different thermal and chemical conditions occur to the aluminum particles close to the burning surface. This study investigates the combustion behavior of aluminum particles in an ADN/GAP matrix in comparison to AP/HTPB at various pressures up to 15 MPa. The agglomeration of Al particles at the surface and burning behavior of aluminized AP/HTPB propellants has already been investigated and is extended to the ADN/GAP propellants. The temperature measurements close to the propellant surface indicate higher values near the Al boiling point that accelerates the melting of Al particles and influences the agglomeration process. At higher pressure the temperatures are in the magnitude of Al_2O_3 evaporation and decomposition close to 3000 K.

V. Weiser (✉) • S. Fischer • V. Gettwert • S. Kelzenberg • S. Knapp • A. Raab • E. Roth
N. Eisenreich
Fraunhofer-Institut für Chemische Technologie (ICT), Energetic Systems, 76327 Pfinztal,
Germany
e-mail: volker.weiser@ict.fraunhofer.de

A. Franzin
Fraunhofer-Institut für Chemische Technologie (ICT), Energetic Systems, 76327 Pfinztal,
Germany

Space Propulsion Laboratory (SPLab), Department of Aerospace Science and Technology,
Politecnico di Milano, 20156 Milan, Italy

L.T. DeLuca
Space Propulsion Laboratory (SPLab), Department of Aerospace Science and Technology,
Politecnico di Milano, 20156 Milan, Italy

1 Introduction

The growing public awareness towards the environment problem, which has driven the last decades of aeronautical research to find a “green fuel,” could not leave out the scope of rocket propulsion. The solid propellant formulations, commonly used for space access until today, contain mostly ammonium perchlorate in combination with hydroxyl-terminated polybutadiene (AP/HTPB). One of the main combustion products is hydrogen chloride (HCl) that should be considered as critical pollution, since it contributes to acid rain and causes environmental damage and corrosion around the launch base. The boosters contain this type of solid propellants, burn in the order of tons per second, releasing large quantities of HCl, which can reach more than 20 % of the reaction products at the nozzle. Also aluminum chloride and other intermediate reaction products, which are not more than 2 %, will cause additional serious problems when the huge quantities of expelled mass are considered.

These are the main motivations to develop a new kind of green propellant that possibly will achieve better propulsive performance as well.

Ammonium dinitramide (ADN) seems to be a promising substitute to ammonium perchlorate, as shown in References [1–3], being chlorine-free. Due to its lower oxygen balance of +25.8 %, instead of +34.04 % for AP, an energetic binder is needed to compensate this handicap. The main problem of ADN is its reactivity with some polymeric binders or at least the ingredients of the polymerisation process [2]. To overcome this problem, coated ADN prills shall be used; for details see [4].

An appropriate binder is GAP (glycidyl azide polymer), an energetic polymer treated with bis-propargyl-succinate and isocyanates (Ref. [5]). Using GAP diol less oxidizer is needed and allows higher Al filler contents than HTPB to increase specific impulse.

Thermodynamic calculations of the theoretically delivered mass specific impulse under frozen equilibrium assumption are presented in Fig. 1 to compare the system ADN/GAP/Al with the established system AP/HTPB/Al. The calculations were performed using ICT-Thermodynamic Code for an expansion ratio 70:1 [6]. It is noticeable that the system ADN/GAP/Al features in a significantly higher gravimetric specific impulse with a maximum of 296 s at 59 % ADN, 20 % GAP, and 21 % Al in a wider region of aluminum content in comparison with AP/HTPB/Al (maximum 284 s at 68 % AP, 12 % HTPB and 20 % Al). Even more remarkable is the fact that the compositions with the higher specific impulses are in a region of larger binder contents of 20–30 % instead of 10–20 % for AP/HTPB/Al that will allow to produce such formulations with improved mechanical properties.

The calculations also show that the increment of specific impulse is mainly caused by about 220 K higher adiabatic combustion temperatures, since the variation in the molecular mass of combustion products, considered in the combustion chamber, features in less marked differences as already discussed in [7].

The purpose of this paper is to report investigations of the burning behavior of an ADN/Al/GAP propellant. The decomposition of ADN/GAP takes place at different thermal conditions than AP/HTPB and results in a significantly different

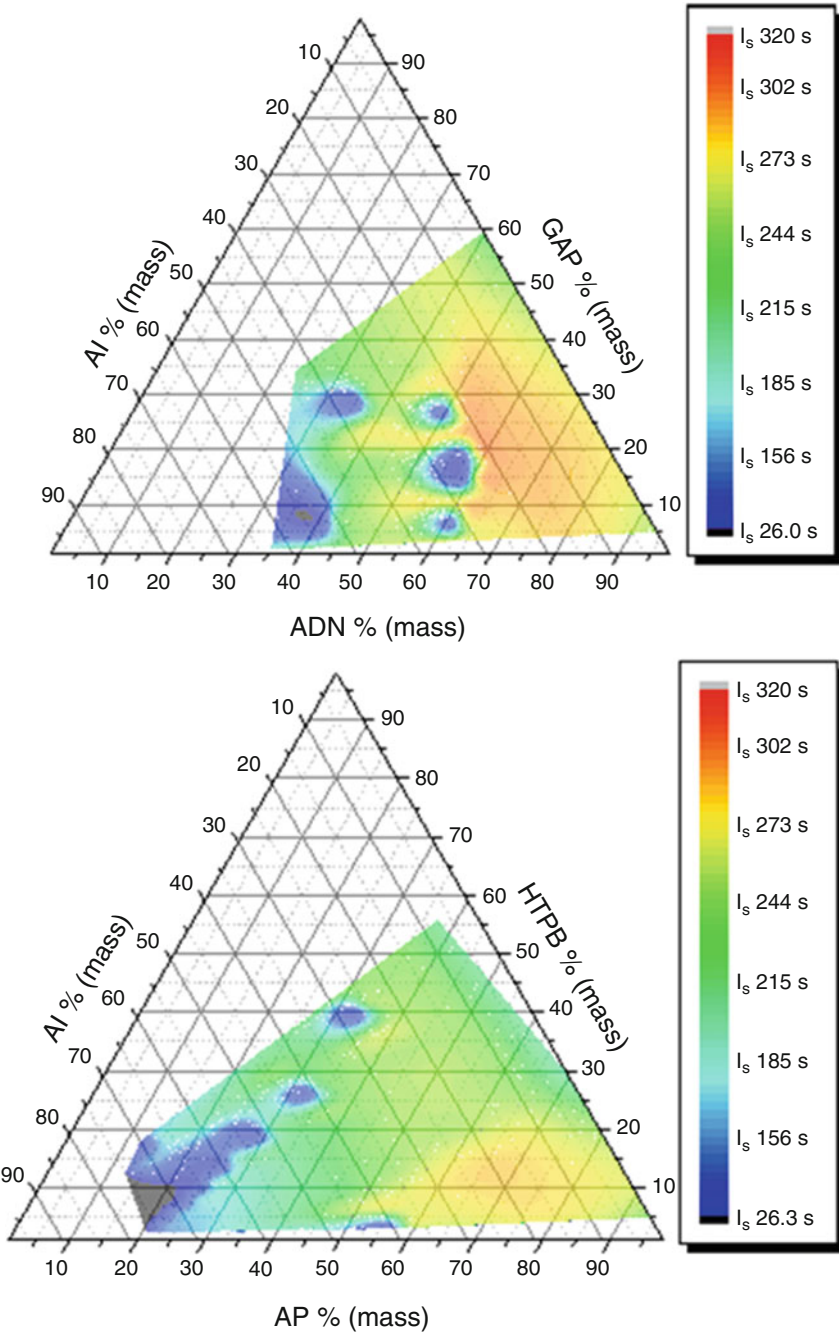


Fig. 1 Comparison between gravimetric specific impulse (frozen equilibrium) of AP/HTPB/Al formulations and ADN/GAP/Al formulations

decomposition product spectrum to oxidize aluminum particles. Based on previous work presented recently [7], this paper describes investigations of the agglomeration of Al particles on the burning surface, the resulting solid residues, the burning rates, and the temperatures depending on the pressure.

2 Experimental

2.1 Tested Formulation

A propellant formulation called H32 was prepared with the composition listed in Table 1 including aluminum particles of 18 μm . Prilled ADN was produced by an emulsion prilling method at ICT, starting from neat ADN delivered by Eurenco Bofors with a particle size distribution for ADN 208 μm of d(0.1) 122 μm , d(0.5) 208 μm and d(0.9) 349 μm and ADN 55 μm of d(0.1) 33 μm , d(0.5) 55 μm and d(0.9) 100 μm [4]. GAP diol prepolymer ($M_n = 1685$, $M_w = 1909$, equivalent weight 1160 g/mol) was purchased from Eurenco (France) and the isocyanate curing agent Desmodur E305 (equivalent weight 328 g/mol) from Bayer Material Science (Germany); and the alkyne curing agent bis-propargyl-succinate (BPS, equivalent weight 97 g/mol) was synthesised from succinic acid (Merck 822260) and propargyl alcohol (Merck 807050) by ICT. The curing catalyst dibutyltin dilaurate (DBTDL) was bought from Merck Schuchardt (8.20421.0250).

A quite large amount of 16 % aluminum with a mean particle size of 18 μm was chosen to achieve an optimum value of specific impulse of 2695 Ns/kg (4676 Ns/dm³) for 7–0.1 MPa expansion. The vacuum specific impulse is calculated to 293.7 s using ICT-Thermodynamic Code.

The ingredients were mixed in a planetary centrifugal vacuum mixer (Thinky mixer ARV-310) with 1600 cycles per minute at a pressure of 3500 Pa for 2 min. GAP diol was added into a beaker and mixed with DBTDL and aluminum, followed by ADN prills in a bimodal distribution 70:30 with an average diameter of 208 μm for the coarse prills and 55 μm for the fine prills. The mixture was cooled down to room temperature. E305 and BPS were added together to the dispersion. The mixing and casting of propellant sheets proceeded without any problems. From the sheets, propellant strands of 4 × 4 × 35 mm³ were cut for combustion tests.

A sample density of 1.641 g/cm³ was measured using He-pycnometer method. This corresponds to a porosity of 3.70 % related to the measured densities of the individual ingredient.

Table 1 Composition of Al/ADN/GAP

ADN ^a	GAP diol	E305 ^b	BPS	Al	DBTDL ^c	NCO/OH ^c
60 %	19.59 %	3.1 %	1.31 %	16 %	0.04 %	0.56

^aPrills 208 μm and 55 μm – ICT Fraunhofer

^bDesmodur

^cCatalysts are not included in final formulation

2.2 *Experimental Setup*

The combustion behavior was investigated in the ICT window bomb under 0.1, 0.5, 1, 3, 5, 7, 10, 13, and 15 MPa nitrogen. The chimney-type pressure vessel is equipped with four windows where glasses of different types of material can be inserted, to allow spectroscopic investigations in the UV, Vis, NIR, and MIR range. Ignition was performed using a fuse wire enhanced with about 50 mg of a booster mixture. Partially an inhibitor on the lateral surfaces of the strands was used. But no significant difference in the burning rate with and without inhibitor was found.

In order to collect aluminum particles, a SEM sample holder was positioned above the strands inside the window bomb, at various distances (from 5 to 15 mm in dependence on observed flame length) from the upper surface of the strands. To preserve the sample holder from the possible contamination of the booster mixture, the strands were ignited using only the fuse wire. The particle collection was carried out at all pressure levels under investigation.

2.3 *Measurement Techniques and Data Evaluation*

To visualise the propellant combustion, a 24-bit color high-speed camera (Motion-ProTM X-3, Redlake) equipped with a 105 mm macro lens was used. The maximum resolution is 1280×1024 pixel. It can be used up to a recording frequency of 2000 fps. By reducing the image section, a maximum frequency of 64,000 fps is possible. The procedure reported in [8] was used to determine steady-state, linear burning rates.

To study the size and behavior of the agglomerates near the surface of the burning propellant, the video records were analysed manually picture by picture taking the sizes of all well-defined and detached particles, as explained in [9]. In combination with the optical imaging, an image resolution of about $14 \mu\text{m}$ per pixel was achieved. The pressure domain of investigation was 0.1, 1, 3, and 5 MPa.

The particles collected on the sample holders were studied using a field emission scanning electron microscope (FE-SEM, Zeiss Supra 55 VP). Elemental composition close to the surface was analyzed by energy-dispersive element analysis (EDX).

While the propellant strand is burning down, material from different flame zones is deposited in layers on the sample holder with material of the flame zone closest to the surface as the lowest layer. In order to investigate also this material, the total sample was transferred head-down to another sample holder.

NIR spectra from 1.0 to $2.2 \mu\text{m}$ were measured using an MCS 611 PGS-NIR 2.2 spectrometer from Carl Zeiss AG, Germany, equipped with an optical fiber with a temporal resolution up to 70 Hz. The spectra were calibrated using a black body radiator in intensity units versus unit wavelength. To limit the field of view of the spectrometer optics, a 2 mm slit diaphragm was fixed about 15 mm distant from the propellant strand. So a local resolution of about 2–3 mm can be estimated. Each spectrum was analyzed by ICT-BaM code that does not require absolute

spectral radiance to derive temperatures from NIR because it models spectra of gaseous reaction products, soot and continuum radiation only based on their band shapes. The evaluation procedure uses a least squares fit of calculated spectra to the measured ones. The technique is described in [10].

3 Results and Discussion

3.1 Visible Observations and Burning Rate

The propellant strands ignited and burnt steadily at all considered pressure levels. This means pressure deflagration limit (PDL) could not be measured exactly but might be less than or equal to 0.02 MPa, as experimentally realised.

Figure 2 shows pictures that are optimised to visualize hot particles by a strong reduction of exposure time and aperture. At ambient pressure, a small number of distinguishable particles with rounded shape stand on the propellant surface. Occasionally single, mainly larger, particles detach and lift off. With increasing pressure, the number of lift-off particles increases drastically, but the shape of a single particle gets more and more diffuse, and they become smaller. Above 5 MPa the glowing particle density increases to form a cloud because the length of the zone of glowing particles reduces (as is found for flames with increasing pressure). Dark vapor clouds and particles are ejected as well.

At 1 MPa the number of agglomerated particles on the surface increases compared to 0.1 MPa but seems to decrease in number and size with further increasing pressure. Simultaneously, the brightness of the particles reduces compared to the ones lifted off into the flame zone.

Evaluation of most high-speed movies with AVICOR [8] results in linear burning rates as illustrated in Fig. 3 that show regression plots. At higher pressure a coating

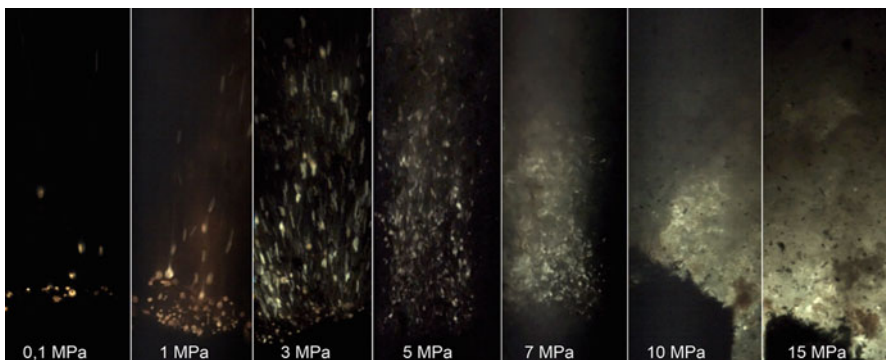


Fig. 2 Selected frames of high-speed movies taken from the combustion of the investigated propellant at various pressure levels

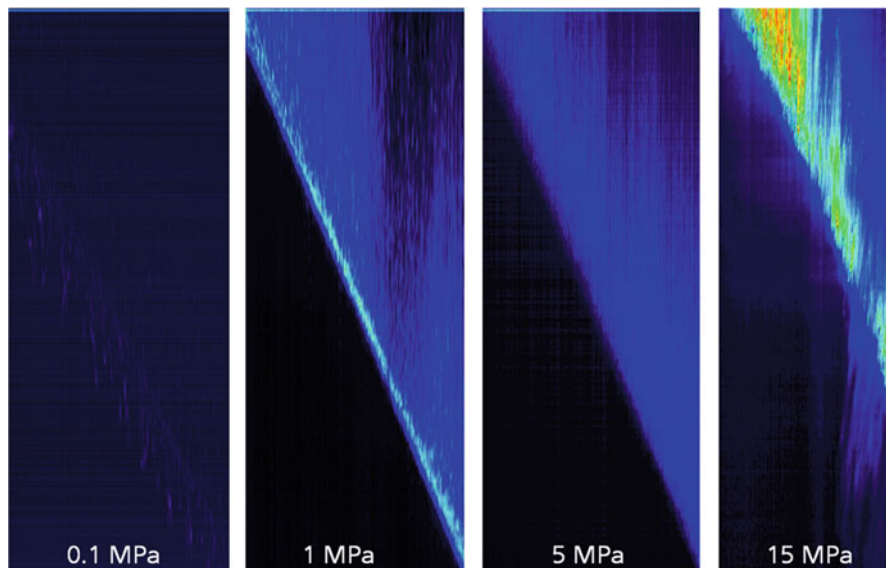


Fig. 3 Regression curves at various pressure levels

consisting of a thin layer of polyurethane was useful to decrease the number of tests failed by lateral combustion. When neglecting failed tests, no other significant differences in burning behavior were found between coated and non-coated strands.

Resulting burning rates are plotted in Fig. 4. On each pressure level 2–6 tests were performed (black dots). Burning rate at 7 MPa is 29.6 mm/s. The mean values of each pressure level can be described in good agreement using a Vieille fit (green line). Vieille fit results in a pre-exponential factor of $A = 8.82 \pm 0.02$ mm/s and a pressure exponent of $n = 0.58 \pm 0.02$ with a coefficient of determination of $R = 0.9956$. The resulting burning rates are quite high for some space applications, but seem applicable to many rocket propulsion applications.

3.2 Spectroscopic Investigations and Temperature

In the wavelength range 0.3–2.15 μm , the spectral emission is dominated by continuum radiation emitted from hot condensed materials. In NIR range water band overlaps the continuum at 1.3–1.6 μm and 1.7–2.1 μm . Additional strong lines at about 769 nm (which is formed from the two lines at 766.4 and 769.8 nm) and 1.17 and 1.25 μm indicate potassium residues in ADN. The strong potassium line is hardly to avoid in engineered propellants especially as ADN is derived from potassium dinitramide. A typical spectrum is plotted in Fig. 5. A view to Fig. 2

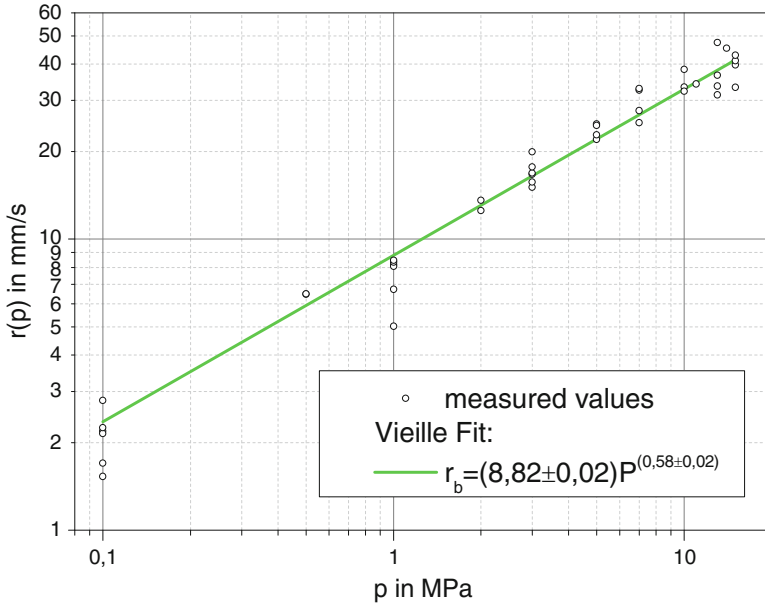


Fig. 4 Burning rate depending on pressure including Vieille analysis

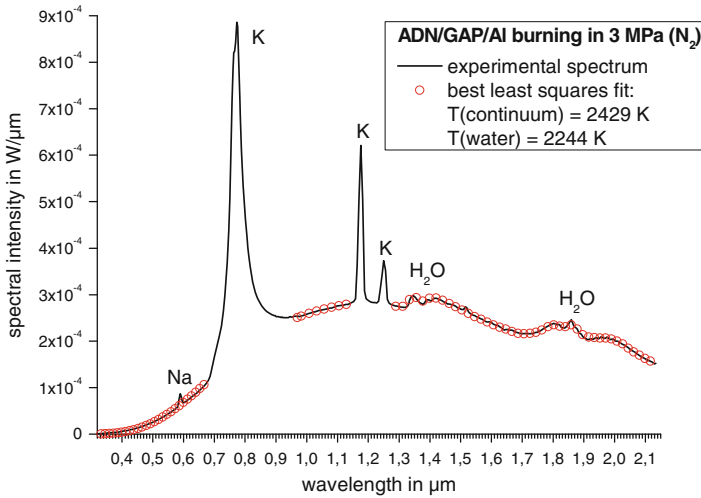


Fig. 5 Characteristic emission spectrum of investigated ADN/GAP/Al propellant including least squares fit by ICT-BaM evaluation combining a grey body continuum with water vapour emission with different temperatures

reveals that the reacting particles emit much brighter than the propellant surface so it is obvious that the continuum spectra can be assigned to the emission of the reacting particles. The main emission is therefore from the reacted caps (or shell) at the aluminum particles which is mainly alumina. The water bands are emitted by water vapour and represent the hot flame gases that emit independently from the particles with possibly a different temperature. Therefore an ICT-BaM analysis may evaluate different temperatures for the continuum and the water bands [10]. To calculate the continuum, grey body emission was applied. Particle clouds might tend to grey body continua because of multiple reflections in a particle cloud. It is difficult to identify detailed wavelength dependence of the continuum additional to it [11]. These evaluations by fitting a calculated spectrum (red dots) consisting of a grey body continuum overlapping with water bands assuming different temperatures to each measured one (black line) agree well when omitting the potassium lines as also shown in Fig. 5. However, in many cases the water bands were too weak to evaluate a reliable temperature. Due to the weak signal intensity, large inaccuracies of the water temperature values are expected.

The water vapor temperatures varied about 200 K around 2000 K. The measured temperatures of the hot particles can be considered as much more accurate and are mainly discussed in the following sections. Figure 6 plots the maximum temperatures measured at each test as a function of pressure (red dots). The values increase drastically from about 2000 K at environmental pressure up to values close to 3000 K at pressures above 10 MPa. Figure 6 also presents the adiabatic temperature calculated using ICT-Thermodynamic Code [6] in the same pressure range that increases from 3100 K at 0.1 MPa to 3600 K at 15 MPa (red line). This

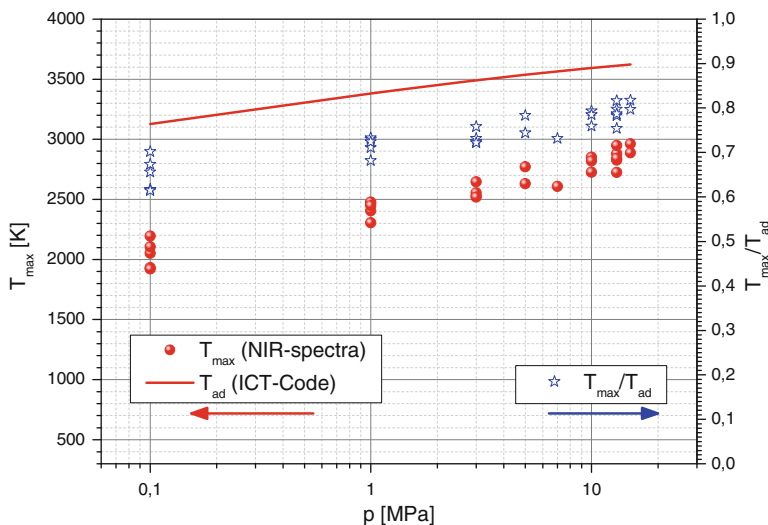


Fig. 6 Comparison of measured maximum temperature and adiabatic temperature calculated by ICT-Thermodynamic Code and their quotient as function of pressure

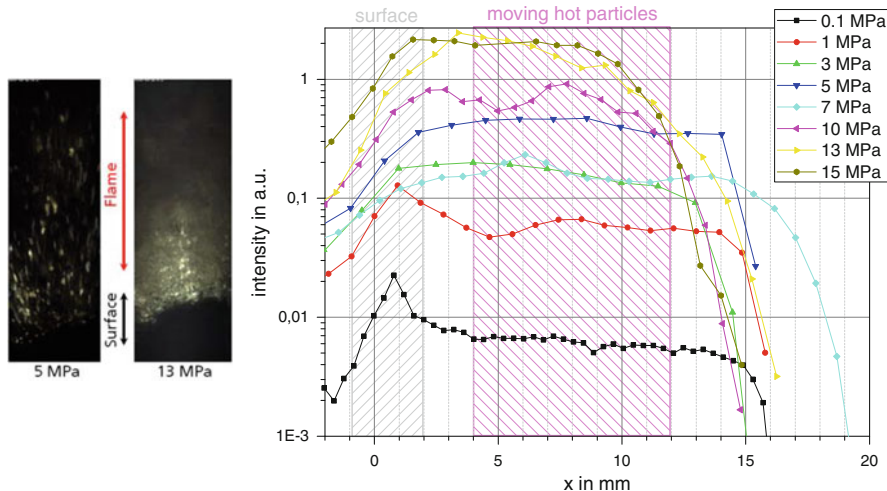


Fig. 7 Axial intensity profiles at various pressure levels

means that the values measured in the window bomb are 30–20 % lower than the theoretical ones, a result which is not unexpected [10]. Regarding the nonadiabatic conditions inside the window bomb and the relatively high absolute temperature values that cause large heat losses, this result seems very reasonable. The ratio of each measured maximum temperature T_{\max} to the adiabatic temperature T_{ad} is also plotted in Fig. 6 (blue stars).

Due to the limitation of the field of view of the spectrometer optics using a slit of 2 mm, the single spectrum can be allocated to different zones along the flame. This can effectively be done using the intensity of the spectra series. According to Fig. 2, there should be a steep increase of intensity close to the propellant surface. This can be detected in the course of the integrated spectral intensity as shown in Fig. 7 (left). The profiles are converted from time t to location x scale using the individually measured burning rate r : $x = r t$. The resolution of the slit of less than 3 mm, as determined above, is in good agreement to the rise of the displayed intensity profiles that should be nearly a jump in reality. So only two flame zones shall be considered: (1) a zone close to the surface where agglomeration takes place and (2) the zone including the moving hot particles. These zones are sketched in Fig. 7. It is assumed that in the second zone, the detached aluminum-rich particles are oxidised by flame gases like water and carbon oxides [12].

At low pressure up to 1 MPa, a peak maximum of intensity is detected close to the surface that can be allocated to the hot particles hovering on the propellant surface. The low intensity of the flame zone may be explained by relatively few particles observed in this range (see Figs. 2 and 7 (right)). With increasing pressure, the peak close to the surface disappears and the maximum intensity is emitted by the flame zone.

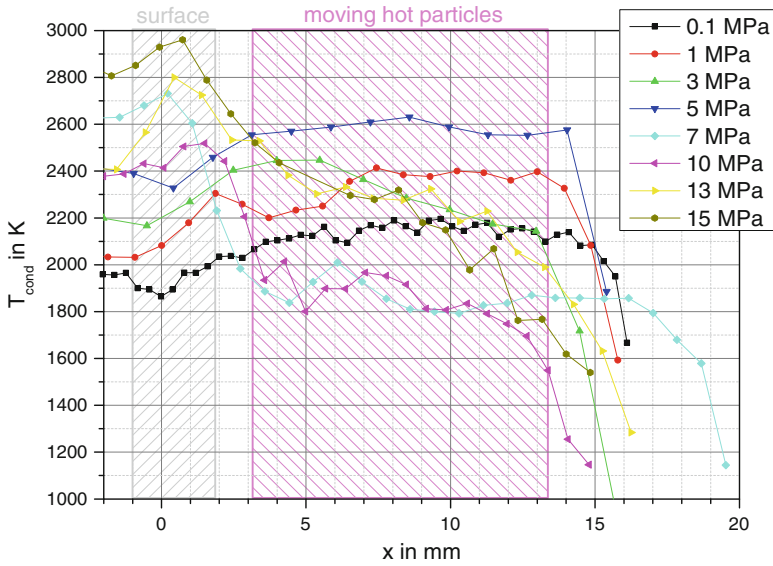
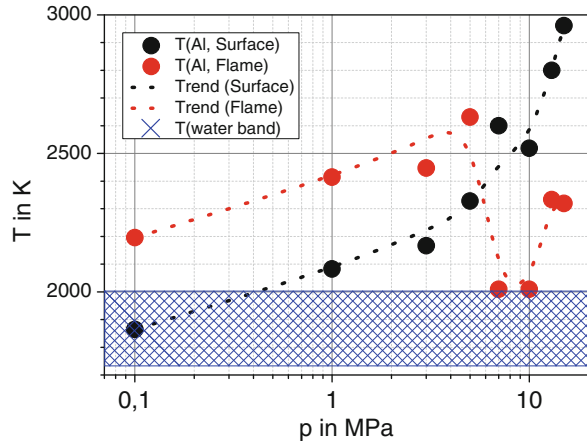


Fig. 8 Axial profiles of continuum temperatures at various pressure levels

The temperature profiles run with an opposing trend. Exemplary curves are shown in Fig. 8. At low pressure up to 5 MPa, the temperatures are lower than the temperature in the flame zone. Above 5 MPa the temperature close to the surface is distinctly higher as inside the flame zone. It is noticeable that independent of pressure, most temperature profiles end at about 15 mm above the surface. This is the position where the particles finish glowing. That means that the velocity of the reaction process increases in a way that it overcompensates the increasing gas flow caused by pressure dependence of burning rate and therefore the flame shifts toward the burning surface. The oxidation zone of the particles shifts in a similar way and produces the temperature maximum close to the surface.

Figure 9 displays the values of measured maximum temperatures in the considered regions as a function of pressure. Close to the surface, the absolute temperature increases drastically from about 1850 K at 0.1 MPa to nearly 3000 K at 15 MPa. Below 5 MPa the temperature of the flame zone is higher and increases from 2200 K at 0.1 MPa to about 2650 K at 5 MPa. Above this pressure, very low values of about 2000 K were observed that increase again above 10 MPa. This might be a result of high optical thickness with increasing particle density that only allows detecting emission from the outer cloud zone.

Fig. 9 Temperatures measured close to the surface and in the flame zone as a function of pressure



3.3 Agglomeration

Using video analysis, it was possible to measure the mean size of the visible particles at the first appearing on the propellant surface. It seems not strongly affected by pressure. The measured average diameter of this kind of particles is around $80 \mu\text{m}$ and is the same at 0.1 and 1 MPa. This value is four times larger than the original aluminum particle size in the formulation. These primary particle agglomerations drastically increase in volume before detaching the surface. Visible observations of the agglomerates show a billowing behavior that indicates liquid state of the particles.

The observed aggregation phenomena for the investigated ADN/GAP/Al formulation can be subdivided in the following five steps:

1. Pre-aggregation inside the condensed phase which results in an increase of aluminum particle diameter from $18 \mu\text{m}$ to the measured $77\text{--}78 \mu\text{m}$ in average.
2. Rising of the pre-aggregated particles on the burning surface and possibly first ignition.
3. Local aggregation with nearest or underlying particles and completion of the transition between aggregates and agglomerates, presenting the well-known oxide cap
4. Rolling of the particles on the burning surface which can result in further aggregation with other rolling particles, but often no aggregation could be observed because of growing volume.
5. When the particles reach a certain diameter, they detach from the burning surface. In many cases the increase of diameter comes along with an increase of brightness that indicates rising temperature. Especially with increasing pressure, some agglomerates are also bloating and seem to boil.

In all observed mixtures, sometimes emerged particles disappear again into pores of the burning strand.

The agglomerates that result from the process of aggregation/agglomeration do not differ so much from the ones observed in AP/HTPB/Al, in fact they seem to be mostly round presenting the same cap of oxide (with some minor exceptions) typical for AP/HTPB/Al propellants (Ref. [13]). After liftoff they show the same turning movement passing the flame zone in a straight line.

The agglomeration size of detaching particles features a quite narrow distribution of diameters with a maximum decreasing with pressure (Fig. 10). In general nearly 2000 particles were metered per histogram. They could be described satisfactorily using a normal distribution for parametric characterisation.

The mean diameters of the analysed detached agglomerates are summarised in Fig. 11 for the investigated sample H32. The agglomerates grow by one order of magnitude with respect to the original size of 18 μm of the aluminum particles. The values decrease from about 265 μm at ambient pressure to less than 150 μm at 5 MPa. This trend is in a good agreement with findings in [14, 15] for the system AP/Al/HTPB.

The sample H32 contains a bimodal size distribution of ADN prills with mean diameters of 208 and 55 μm . In Fig. 11 further results of ADN/Al/GAP formulations with the same composition but with different ADN prill sizes were included [7]. Sample D contains smaller aluminum particles of 5 μm .

As reported in [7] and confirmed by some further investigations of the propellant D and G presented in Fig. 11, the initial dimension of aluminum particles seems not to affect the agglomerate diameter.

The dimension of ADN oxidiser affects the size of agglomerates more significantly. This is also in accordance with observations made for AP/Al/HTPB propellants in [16, 17]. Like depicted in Fig. 11, the biggest ADN prills (H27) correspond to the largest mean size of agglomerates. Although these prills are only 10 % larger (20 μm), the agglomerates are nearly twice as large as those of sample G. Except for 0.1 MPa, the bimodal distribution gives rise to agglomerates which are in between the two monomodal mixtures investigated.

3.4 SEM/EDX Analysis of Collected Particles

Figure 12 presents a selection of SEM images of collected residual particles at different pressures and magnification factors.

Most particles are round. Some especially large particles still feature an oxide cap that indicates an incomplete combustion (Fig. 12a). This is confirmed by EDX analysis with high aluminum-to-oxygen ratios inside the smaller cap. In general, the ratio of O/Al increases significantly with increasing pressure indicating a more complete oxidation. Some EDX analyses, especially taken at 7 MPa and higher, result in additional contents of nitrogen of 10–20 mol%. In many cases these are accompanied by carbon in the same order of magnitude. It is not clear if the nitrogen

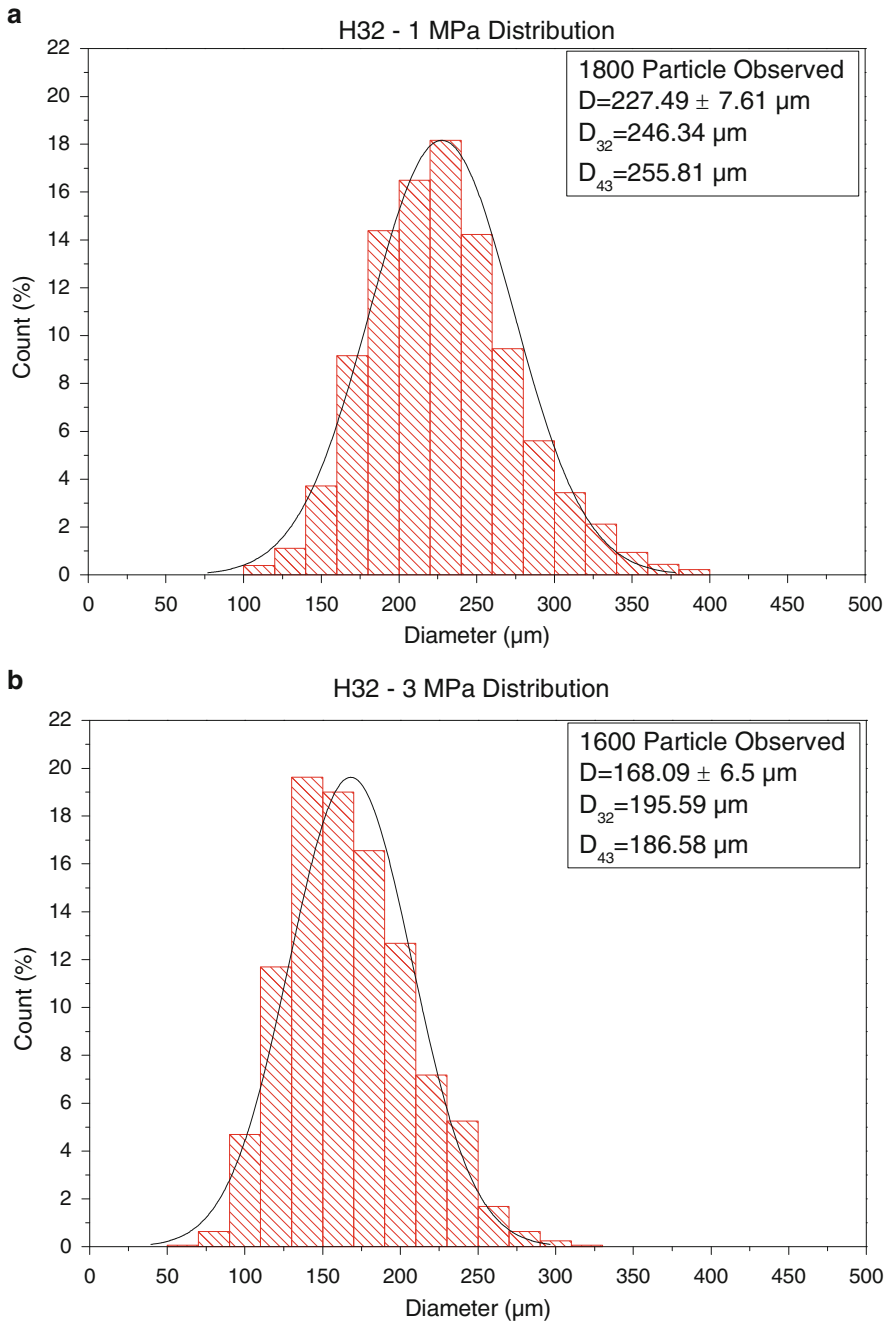


Fig. 10 Histogram of mean diameter for the propellant H32 at (a) 1 MPa and (b) 3 MPa

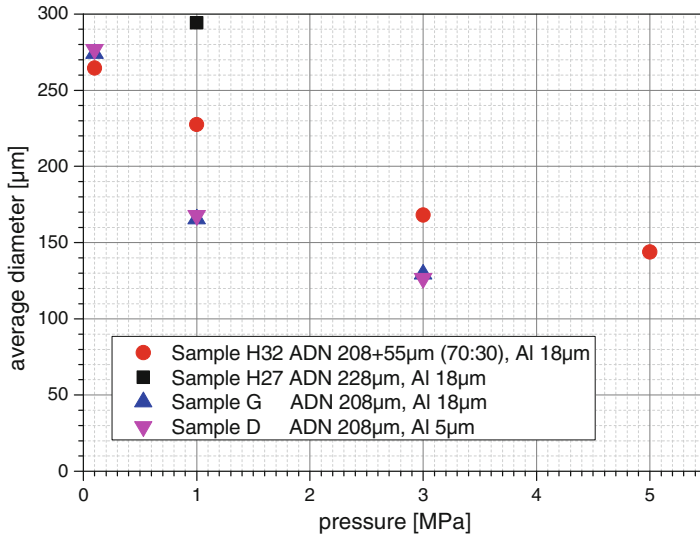


Fig. 11 Mean diameters of agglomerates for different prill sizes of oxidiser

is caused by the components of the formulation (ADN, GAP) or by the reaction with the pressure gas. In the future these investigations will be repeated under argon. But carbon can only be introduced from the GAP binder.

At low pressure 0.1 MPa, many particles with dimensions around 10 µm were found (Fig. 12b). This is in contrast to the agglomeration analysis in Fig. 11. These particles are completely spherical and feature high oxygen content that indicates pure alumina proven by EDX analysis. Maybe small aluminum particles oxidise completely below or at the surface at lower temperatures and are not visible as glowing agglomerates in the movie images. At 0.1 MPa also nanostructures of fluffy material could be observed (Fig. 12). With increasing pressure these structures disappear.

At higher pressure the collected particles consist in spherical sub-particles that look like sintered together to larger aggregates (Fig. 12g, h). This clearly indicates less viscosity probably due to higher temperatures when clashing together.

Most particles collected at all pressure levels show holes, which look like pores formed by gas released from the particle. Also the particles removed from the sample holder’s surface feature in a high number of small frozen bubbles inside (Fig. 12d, e). In some cases also broken hollow spheres were found with only a thin oxide shell (Fig. 12f). This is in accordance to observations of Babuk who also found agglomerates including gaseous enclosures for AP/HTPB/Al propellants [18].

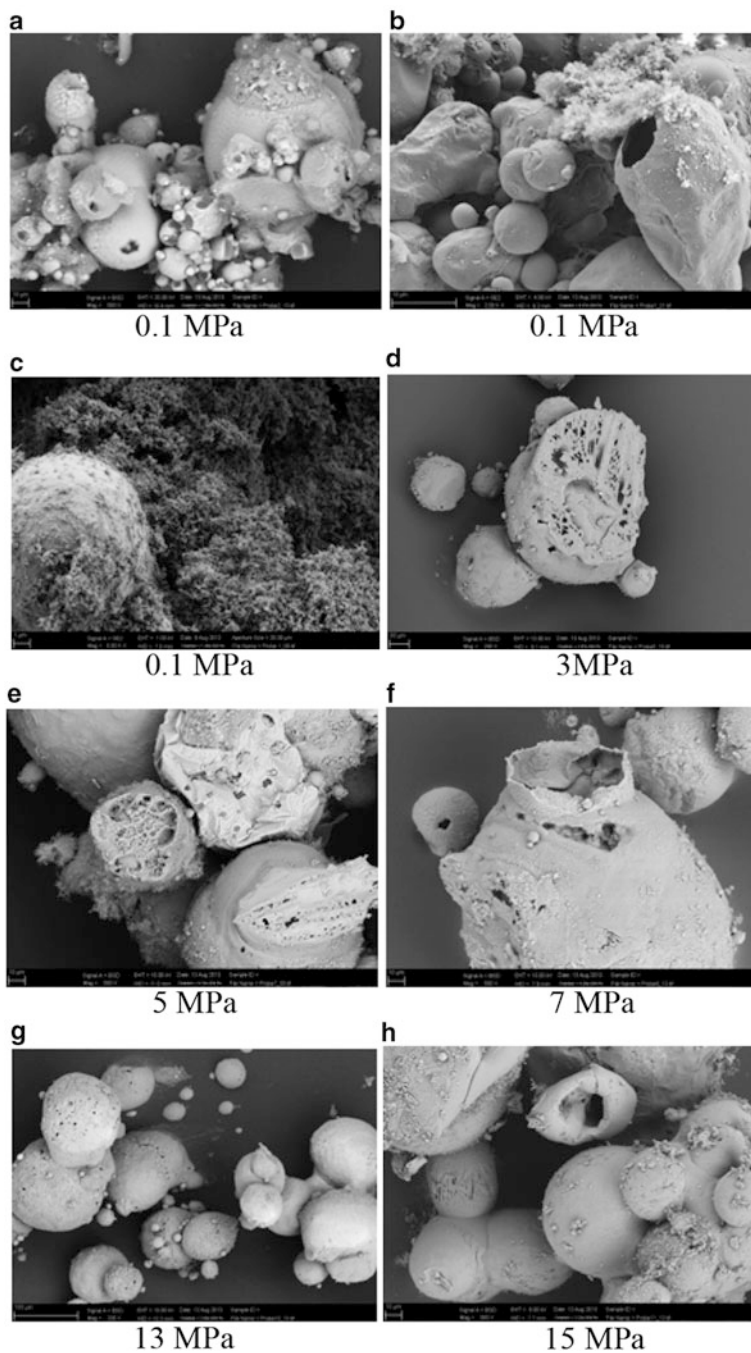


Fig. 12 SEM images of collected products taken at different pressure. (a) 0.1 MPa (b) 0.1 MPa (c) 0.1 MPa (d) 3 MPa (e) 5 MPa (f) 7 MPa (g) 13 MPa (h) 15 MPa

4 Conclusion

The combustion behavior of a formulation including ADN/GAP filled with 16 % aluminum was characterised with a distinct focus on the behavior of agglomerating and reacting aluminum. The propellant features in a pressure-depending burning rate obeying the Vieille's law with a pressure exponent of 0.58 and an A-factor of 8.82 mm/s that is quite high for many applications in space propulsion. Further efforts are necessary to reduce the absolute burning rate. Depending on pressure, very high temperatures up to 3000 K were determined. The agglomeration of reacting aluminum particles behaves similar to the much better investigated system of AP/HTPB/Al. The agglomeration size is mainly influenced by the oxidiser particle size and decreases with increasing pressure. This correlates well with increasing temperatures of the agglomerates close to the surface. The agglomerates do not lift off before reaching a certain size. This contradicts to the physical experience that smaller particles are easier carried as larger ones by a gas flow of a certain velocity and can only be explained assuming a decreasing density during the agglomeration process accompanied by particle oxidation from pyrolysing gases of decomposing ADN/GAP. But the density of pure aluminum of 2.7 g/cm³ is lower than that of oxidised alumina (Al₂O₃: 3.94 g/cm³). So a decreasing density during the oxidation process can only be explained assuming gas enclosures inside the agglomerates like found in the residual particles collected from the flame zone.

Aluminum has a melting point of 934 K and boils at 2743 K at standard pressure. The melting point of alumina (Al₂O₃) is 2345 K and at about 3250 K it boils and decomposes. The measured temperatures of agglomerates on the surface are in the magnitude of boiling aluminum and could be one explanation of gas bubbles inside the particles by aluminum vapour. But also the internal formation of gaseous AlO should be considered.

These phenomena will be the focus of further investigations.

Acknowledgements The research leading to these results has received funding from the European Union Seventh Framework Programme (FP7/2007–2013) under grant agreement no 262099.

References

1. Larsson A, Wingborg N (2011) Green propellants based on ammonium dinitramide (ADN). In: Jason Hall (ed) *Advances in spacecraft technologies*. InTech, Rijeka, Croatia
2. Menke K, Heintz T, Schweikert W, Keicher T, Krause H (2009) Formulation and properties of ADN/GAP propellants. *Propellants Explos Pyrotechnics* 34:218–230
3. Weiser V, Eisenreich N, Baier A, Eckl W (1999) Burning behaviour of ADN formulations. *Propellants Explos Pyrotechnics* 24:163–167
4. Heintz T, Pontius H, Aniol J, Birke C, Leisinger K, Reinhard W (2009) Ammonium dinitramide (ADN) – prilling, coating, and characterization. *Propellants Explos Pyrotechnics* 34:231–238
5. Keicher T, Kuglstatler W, Eisele S, Wetzel T, Krause H (2009) Isocyanate-free curing of glycidyl azide polymer (GAP) with bis-propargyl-succinate (II). *Propellants Explos Pyrotechnics* 34:210–217

6. Volk F, Bathelt H (1998) User's manual for the ICT-thermodynamic code, vol 1, Bericht 14/88. Fraunhofer-ICT, Pfinztal
7. Weiser V, Franzin A, Gettwert V, DeLuca LT (2013) Combustion of metallised ADN/GAP solid rocket propellants with focus on agglomeration effects. In: 5 EuCASS-Propulsion Physics, Munich, 01–05 July 2013
8. Weiser V, Ebeling H, Weindel M, Eckl W, Klahn T (2004) Non-intrusive burning rate measurement under pressure by evaluation of video data. In: 35th international annual conference of ICT, 29 Jun–2 Jul 2004, Karlsruhe, pp 158-(1-6)
9. DeLuca LT, Galfetti L, Maggi F, Colombo G, Reina A, Dossi S, Consonni D, Brambilla M (2012) Innovative metallized formulation for solid or hybrid rocket propulsion. *Chin J Energetic Mater* 20(4):465–474
10. Weiser V, Eisenreich N (2005) Fast emission spectroscopy for a better understanding of pyrotechnic combustion behaviour. *Propellants Explos Pyrotechnics* 30:67
11. Lynch P, Krier H, Glumac N (2010) Emissivity of aluminum-oxide particle clouds: application to pyrometry of explosive fireballs. *J Thermophys Heat Transf* 24(2):301–308
12. Beckstead MW (2004) A summary of aluminum combustion; NATO Report RTO-EN-023; NATO Research & Technology Organization: Neuilly-sur-Seine, France
13. Babuk VA, Vasilyev VA, Malakhov MS (1999) Condensed combustion products at the burning surface of aluminized solid propellant. *J Propuls Power* 15(6):783–793
14. DeLuca LT, Marchesi E, Spreafico M, Reina A, Maggi F, Rossetini L, Bandera A, Colombo G, Kosowski BM (2010) Aggregation versus agglomeration in metallized solid propellants. *J Energetic Mater Chem Propuls* 9(1):91–105
15. Sambamurthi JK, Price EW, Sigman RK (1983) Aluminium agglomeration in solid-propellant combustion. *AIAA J* 22(8):1132–1138
16. DeLuca LT (2007) Burning of aluminized solid rocket propellants: from micrometric to nanometric fuel size, vol VI, Theory and practice of energetic materials. IASPEP, Xi'an
17. Cohen NS (1983) A pocket model for aluminium agglomeration in composite propellants. *AIAA J* 21(5):720–725
18. Babuk VA, Dolotkazin IN, Glebov AA (2005) Burning mechanism of aluminized solid rocket propellants based on energetic binders. *Propellant Explos Pyrotechnics* 30(4):281–290